Optimising a Myocardium-like Hydrogel for Enhanced Cardiomyocyte Culture

Naviya Gupta[1], Dr. Shery Huang[2], and Jack Murphy[3]

[1]**Newnham College, University of Cambridge**
[2]**Cambridge University Engineering Department (CUED)**
[3]**Biointerface@CUED**

ABSTRACT

The prevalence of cardiovascular disease (CVD) worldwide has necessitated the development of physiologically relevant in vitro models for cardiac research and drug discovery. This study investigates the optimization of hydrogel scaffolds for improved synthetic models of the myocardium. Two hydrogel systems—alginate-only and alginate-gelatin blends—were synthesized and tested to determine their mechanical suitability as synthetic cardiac slices. Mechanical testing, including tensile force measurements and Young's modulus calculations, revealed that a 4 % alginate concentration most closely replicated native myocardial stiffness, while higher concentrations were excessively rigid. Acoustic patterning technologies have been used to non-invasively manipulate cells and recapitulate native anisotropic architecture, however, this patterning is quickly lost if not embedded in a suitable hydrogel. The results underscore the critical interplay between hydrogel composition, mechanical properties, and cell alignment in constructing functional in vitro cardiac models. Future work will focus on standardizing gel fabrication, enhancing mechanical characterization, and evaluating cardiomyocyte viability and maturation within these scaffolds, ultimately enabling more accurate modelling of cardiac physiology and pathology.

Keywords: in-vitro, hydrogel, patterning

UNIVERSITY OF CAMBRIDGE

CONTENTS

1 INTRODUCTION

1.1 The Importance of Sources for In-Vitro Studies

Cardiovascular disease (CVD) has long been cited as the leading cause of death globally [10]. CVD is utilised as an umbrella term for disorders related to the heart and blood vessels of the human body. This can comprise coronary (relating to heart muscles) and cerebrovascular disease (relating to blood vessels to the brain), congenital defects and pulmonary embolisms, and numerous other such conditions. The World Health Organization estimates that CVDs claim the lives of around 17.9 million annually, with heart attacks and strokes making up 80 % of these deaths [2].

Developing successful tissue regeneration and drug discovery strategies requires a thorough understanding of the role that mechanobiology plays in cardiac (patho)physiology, which calls for extensive cause-and-effect research. High levels of experimental control are made possible by the creation of three-dimensional in vitro models, which combine insights from in vivo research and complementary cell culture models. These in vitro models will provide prospective perspectives to outline the influence of mechanobiological stimuli on human cardiac (patho)physiology in a dish, supported by the use of human-induced pluripotent stem cells, with or without predisposed genetic disorders [8].

2 BACKGROUND INFORMATION

2.1 Current Methods of In-Vitro Study of Cardiomyocytes

There are two predominant cell sources available for cardiomyocytes: primary cells extracted from heart sample and iPSC-derived cardiomyocytes. Primary source extraction involves isolating cardiomyocytes (CMs) directy from biological heart tissue, sources can include animal source, cardiac biopsies from adult human hearts, or full human hearts from donors. Induced pluripotent stem cells, which are reprogrammed adult somatic cells, produce induced pluripotent stem cell-derived cardiomyocytes (iPSC-CMs), which are heart muscle cells. By offering patient-specific cellular models, these specialized cells are an effective tool for drug development, toxicological testing, and modelling heart disorders [9].

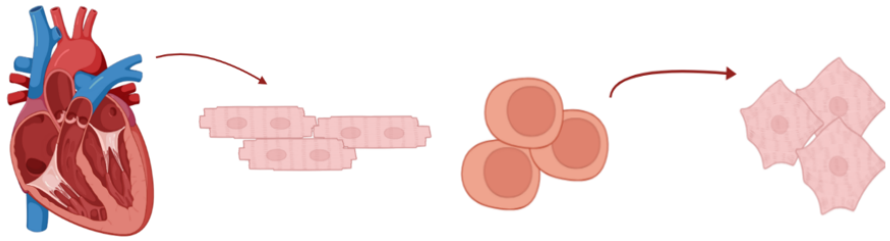

Figure 1. Schematic of Primary Source Cardiomyocytes and iPSC-derived cardiomyocytes created using BioRender [1]

2.2 The Need for Optimization of In-Vitro Study

To replicate the characteristics of native heart tissue, 3D constructs must be engineered using suitable cell sources and biomaterials that closely imitate the native tissue's architecture, support cell survival and function, enable electrical and mechanical integration with the host, and promote blood vessel formation [5].

Primary extraction offers high physiological relevance but are scarce, non-proliferative and lose function in-vitro. Additionally, lack of native tissue cues such as mechanical load, 3D structures and cell-cell interactions limit proper maturation of these cells. Conversely, iPSC-CMs often lack maturity, failing to replicate the structure and function of native heart tissue. These cells remain immature, displaying foetal-like electrical, structural, and metabolic properties even after long-term culture [12].

2.3 Objective of Research

The overarching aim of this study is to develop a hydrogel system that permits acoustic patterning of cardiomyocytes in the precursor, fluid state, while providing sufficient structural integrity post-crosslinking

to preserve alignment and support tissue maturation. These objectives will be achieved using a custom acoustic patterning setup and embeddding CMs in various hydrogel concentrations. Comparative mechanical testing of these hydrogels will be used to assess these hydrogels suitability as a "synthetic cardiac slice" to closely mirror native characteristics.

2.4 Acoustic Patterning Setup and Theory

1. The initial setup is prepared with the acoustic patterning device and medium:
   i. A sterile petri dish is placed onto the acoustic patterning device with transducers attached to either side.
   ii. The pre-warmed alginate-based hydrogel solution (without cells) is added to the dish.
2. The acoustic field is initiated:
   i. The acoustic patterning device is switched on to generate ultrasonic standing pressure waves [11]
   ii. This creates predictable pressure nodes in the pattern of linear fibres within the fluid medium.
3. The cells are introduced into the fluid medium via pipetting:
   i. Cardiomyocytes are carefully added dropwise into the fluid alginate solution. Cells migrate and align along the pressure nodes due to acoustic forces and form line arrangements in accordance with the waves
4. Once the desired cell patterning is achieved, the calcium chloride is gently added to trigger gelation of alginate, crosslinking the hydrogel and thus locking the cells in place.

A limitation of this technique when used without hydrogel is that the acoustic field only maintains the pattern while the standing wave is present. Once the acoustic excitation is turned off, or when the culture dish is disturbed or moved, the patterned arrangement of cells rapidly disperses due to Brownian motion and fluidic perturbations. To overcome this, hydrogels are crosslinked immediately after acoustic patterning. The hydrogel serves as a structural matrix that polymerizes around the patterned cells, effectively "locking" them in place. This ensures that the cellular arrangement generated by the standing wave field is preserved even in the absence of continued acoustic excitation, thus addressing a major drawback of conventional acoustic patterning approaches.

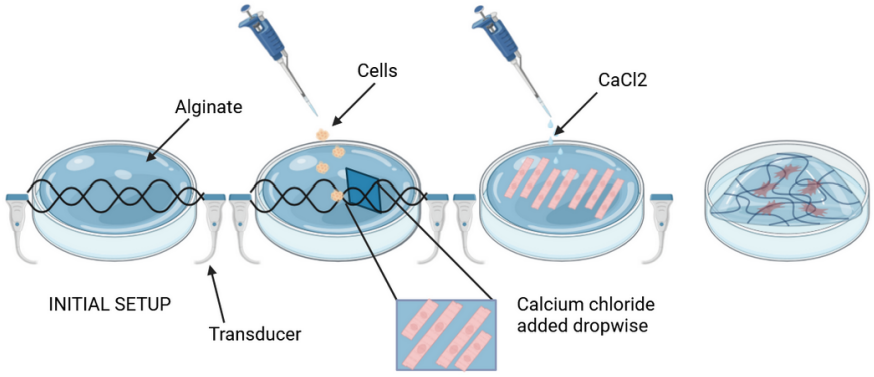

Figure 2. Graphic schematic of the step-by-step procedure for acoustic patterning created via BioRender [1]

2.5 Acoustic Patterning: Cell Arrangements from Previously Conducted Procedures

Acoustic standing waves have been employed to spatially organize cells within hydrogel precursors at two distinct frequencies. At 6.7 MHz, cells aligned into multiple fine bands with regular spacing, forming discrete parallel lines across the field of view (Figure 3, left). Using the 100 μm scale bar, the inter-band spacing was estimated to be approximately 110–120 μm, which is consistent with the expected half-wavelength ($\lambda/2$) for ultrasound in aqueous media at this frequency ($\lambda \approx 220$ μm, $\lambda/2 \approx 110$ μm). Cells were distributed predominantly as single units or small clusters along the nodal lines, indicating precise microscale positioning with high spatial resolution, albeit with lower local cell density within each band.

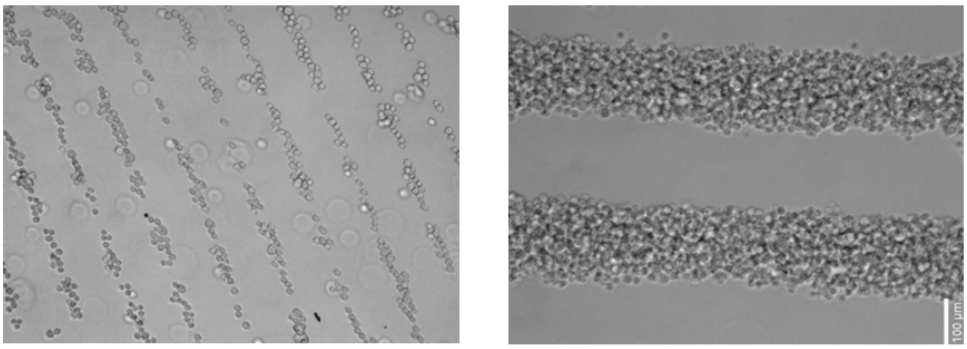

Figure 3. Acoustic Patterning of Cardiomyocytes at 6.7 MHz and 2 MHz Frequency Standing Waves

At 2 MHz with a 30-minute exposure, cells aggregated into broader, denser bands with greater spacing between adjacent regions (Figure 3, right). The measured band spacing was approximately 350–400 μm, again matching the predicted half-wavelength for this lower frequency ($\lambda \approx 740$ μm, $\lambda/2 \approx 370$ μm). Unlike the 6.7 MHz condition, the 2 MHz patterning produced thick, cell-rich regions separated by acellular gaps, forming continuous multicellular bands that more closely resemble tissue-scale structures.

3 METHODOLOGY

3.1 Synthesis of Hydrogels

The objective was to synthesize 2 sets of hydrogels – one solely from an alginate base, and one via a combination of alginate and gelatin. The purpose of this was to investigate the effect of these different compositions on the setting of cardiomyocytes – where the hypothesis was that the alginate-only trials would result in the cardiomyocytes binding to each other, whereas the alginate-gelatin sample might encourage the cells to bind to each other as well as the hydrogel. This phenomenon is desired as it attempts to reform cell junctions between cardiomyocytes. Which case is more desirable would be discovered through further experimentation and acoustic patterning trials.

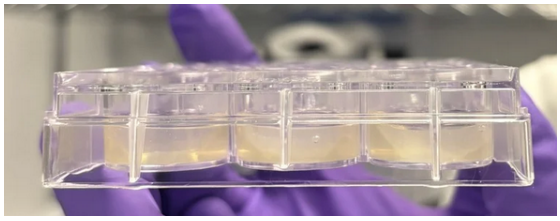

Figure 4. Cross-linked hydrogels forming a concave meniscus in side-view

3.1.1 Materials and Apparatus

The materials and apparatus utilised for this procedure were given as follows:

Magnetic Stirrer	×1
Weighing Scale	×1
Centrifuge	×1
Pipettes	Modifies with trials
Beakers	×3
Experimental Hydrogel Dish	×12 cavities in 1

Table 1. Apparatus Utilized for Hydrogel Synthesis

Alginate $(C_6H_7NaO_6)_n$	1.6 g
Gelatin	1.6 g
Phosphate-Buffered Saline (PBS)	200 mL
Calcium Chloride ($CaCl_2$)	1.76 g

Table 2. Chemicals Utilized for Hydrogel Synthesis

3.1.2 Procedure: Alginate-only Hydrogel

- 3 $CaCl_2$ solutions were prepared by mixing 320, 160 and 80 mL of PBS with 1.76 g of $CaCl_2$, resulting in 50, 100 and 200 mM concentrations
- 3 alginate solutions were prepared as 1.6 g of amorphous alginate was weighed out and added slowly to 160, 80 and 40 mL of PBS buffer solution, resulting in 1%, 2% and 4% concentrations respectively
- The base was then allowed to warm slightly (to 37 °C) before mixing
- The solution was allowed to mix using a magnetic stirrer for approximately 2 hours, allowing the alginate to fully dissolve
- The $CaCl_2$ was then added dropwise to alginate in the compartments of the hydrogel dish and allowed to stand for 5 minutes to facilitate crosslinking. Concentrations 200, 100 and 50 mM of $CaCl_2$ and 1%, 2% and 4% alginate solutions were attempted in order to determine the optimal consistency required to hold the cardiomyocytes during acoustic patterning.

3.1.3 Procedure: Alginate-Gelatin Hydrogel

- 4 different combinations of alginate and gelatin concentrations were synthesized to optimize hydrogel consistency
- 2 % weight by volume of gelatin was prepared via combining with 80 mL of PBS buffer
- The gelatin mixture was allowed to cool as the alginate was being prepared
- In this case, 4 alginate mixtures were prepared – with 4 %, 2 % and 1 % concentrations respectively
- Gelatin solution were added to each of these yielding 1% and 2% concentrations of alginate-gelatin hydrogels

3.2 Mechanical Testing of Hydrogel Samples

3.2.1 Hydrogels as Synthetic Cardiac Slices

This experiment partly hinges on the modelling and testing of hydrogels as synthetic cardiac slices, whereby they are synthesized with different chemical concentrations to find the closest match in mechanical properties [3]. Unlike to isolated myocytes, cardiac slices allow for the study of heart function in a multicellular setting with an entire myofilament lattice. Additionally, slices preserve intercellular signalling and in vivo architecture, which increases the likelihood that experimental findings may have physiological significance. Furthermore, cardiac slices enable tests that are too challenging or impossible to carry out in entire hearts.

3.2.2 Design and Working Principle of Tensile Test Device

For these trials, an IonOptix Cardiac Slice System is used to monitor the tensile force applied vs. stretch (displacement Δ x) [6][3]:

Sturdy, stable triangular clips are used to attach the hydrogel samples that mount between a programmable length controller and a force transducer. Temperature control is made possible by chamber fluid flow. Electrical field stimulation is made possible by fixed platinum electrodes. Platinum minimizes electrolysis, permits electrical conductivity, and is biologically inert.

Force-feedback length control can be used to acquire mechanical work loops produced by cardiac slices (shown in real-time), which are comparable to pressure-volume work loops in the human heart.

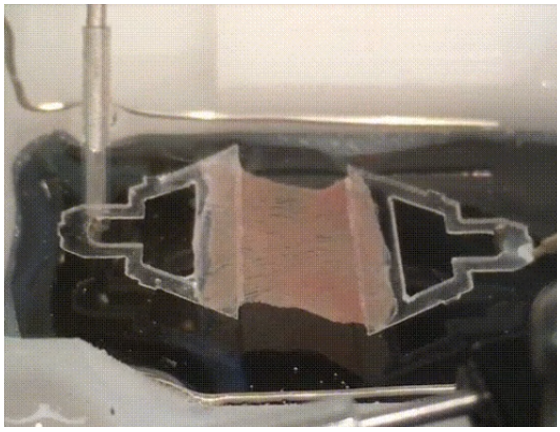

Figure 5. Cardiac slice loaded onto the IonOptix Slice System [6]

Important functional information, such as end-systolic and end-diastolic force-length relationships (ESFLR and EDFLR), which describe the cardiac slices's elastance and compliance as well as mechanical work and power, can be obtained using force-length work loops. The core IonWizard software is used to acquire data for the experiment; trace recordings are used to present length controller position and force data.

3.3 Acoustic Patterning

3.3.1 Design and Setup of Device

The acoustic patterning device (Figure 6) used in this work comprises two piezoelectric transducers mounted on a custom-designed frame. Each transducer is supplied with a sinusoidal voltage signal of approximately 20 Vpp, tuned to its first harmonic resonant frequency (2 MHz). This resonant frequency can be determined either by theoretical calculations, based on the properties of the transducer, or experimentally through frequency sweeps to identify the maximum acoustic output. [11]. When driven at resonance, each transducer produces transverse acoustic waves that propagate through the culture medium. The interaction of these counter-propagating acoustic waves results in the formation of a standing wave field. Standing waves are characterized by periodic pressure nodes (regions of minimal pressure fluctuation) and antinodes (regions of maximal fluctuation). Cells suspended in the medium experience an acoustic radiation force arising from the pressure gradient of this field [13]. The primary acoustic radiation force (F_{rad}) acting on a spherical particle of radius a in a one-dimensional standing wave of wavelength (λ) can be described by:

$$F_{\text{rad}} = -\frac{4\pi a^3 \kappa_m E_{ac}}{\lambda} \Phi \sin(2kx), \tag{1}$$

where K_m is the compressibility of the medium, E_{ac} is the acoustic energy density, $k = 2\pi/\lambda$. k is the wave number, x is the position relative to the pressure node, and (ϕ) is the acoustic contrast factor determined by the relative density and compressibility of the cell compared to the surrounding fluid. For most mammalian cells suspended in aqueous medium, (ϕ)$\geq$0, causing them to migrate toward pressure nodes. As a result, cells accumulate at these nodal positions, forming well-defined, tightly packed bands.

4 RESULTS

4.1 Hydrogel Fabrication

The hydrogels fabricated at different $CaCl_2$ molarities and alginate concentrations are depicted in Figure 7. The hydrogels were also observed on a dark surface so as to show the varying levels of viscosity with molarity and alginate concentration. It was observed that the highest molarity (200 mM) coupled with the highest alginate concentration 4% resulted in the most rigid gel, forming a concave, bowl-like meniscus. In contrast, the lowest molarity (50 mM) yielded very soft gels that lacked structural integrity.

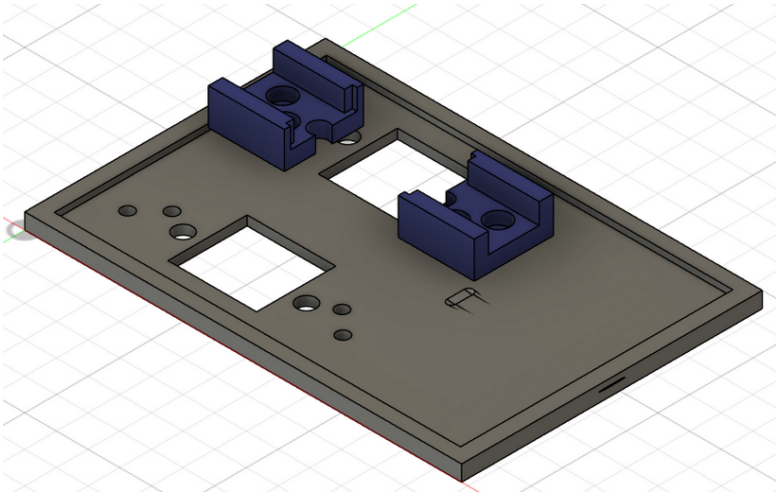

Figure 6. CAD Model (developed on Fusion) for the Acoustic Patterning device with wells for the cells

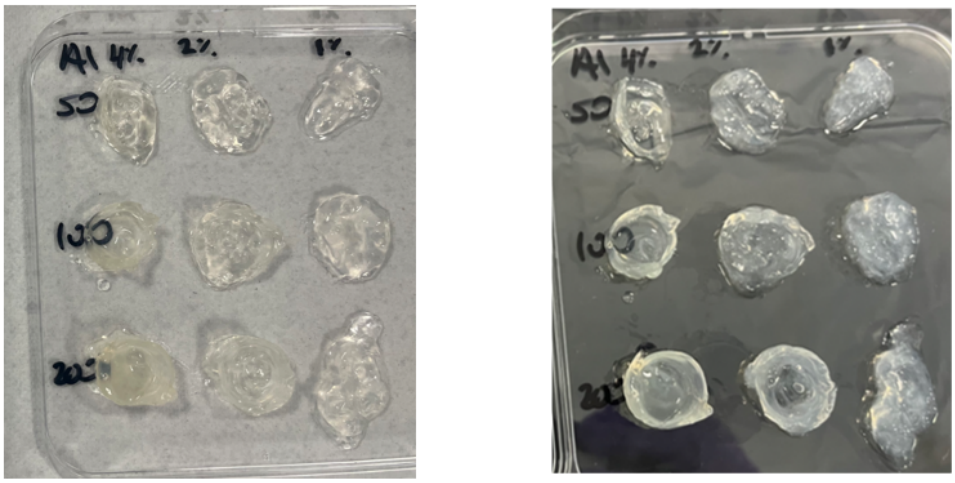

Figure 7. Hydrogels prepared with different concentrations of alginate (4% , 2% and 1%) and $CaCl_2$ 200, 100 and 50 mM

Figure 8 depicts hydrogels synthesized with 2% gelatin added to the alginate mix. The observations in terms of viscosity showed the same patterns as the alginate-only gel, but the inclusion of gelatin seemed to yield less rigid gels that could not maintain a bowl-like structure as well. Additionally, cross-linking seemed to take a longer duration and un-crosslinked solution had to be pipetted out to isolate the gel. This occurs because gelatin dilutes and thus does not cross-link. Hence, it can leak out of the structure if the alginate is not fully cross-linked.

4.2 Mechanical testing: Hydrogel Stress-Strain Curves and Young's Modulus Data

Mechanical testing was used to obtain data for the tensile force exerted on the alginate-only hydrogel samples vs. the change in linear length of the sample due to stretching. The aim was to attain curves of nominal stress vs. nominal strain for the sample to calculate Young's Modulus as a material property for different hydrogel concentrations:

$$\text{Stress} = \frac{\text{Force}}{\text{Area of cross-section}} \qquad \sigma = \frac{F}{A} \tag{i}$$

$$\text{Strain} = \frac{\text{Change in length}}{\text{Original length}} \qquad \varepsilon = \frac{\Delta L}{L_0} \tag{ii}$$

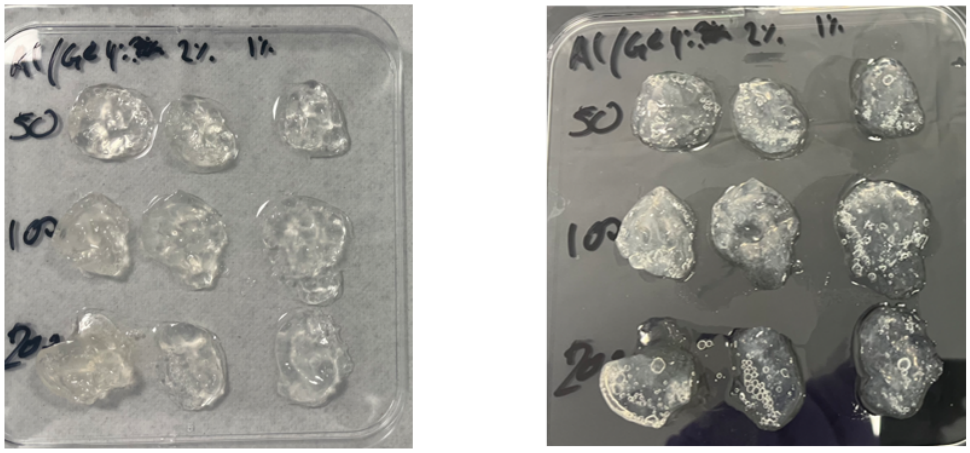

Figure 8. Hydrogels prepared with different concentration of alginate(4%, 2% and 1%)-gelatin(2%) and $CaCl_2$ (200, 100 and 50 mM)

$$\text{Young's Modulus} = \frac{\text{Stress}}{\text{Strain}} \qquad E = \frac{\sigma}{\varepsilon} \tag{iii}$$

This was achieved by running the data through a Python code based on the formulae for conversion of force to stress and change in length to strain.

1) Alginate Hydrogel Trial 1: 200 mM 8% concentration of alginate

Strain	Stress	Displacement (mm)	Force (mN)
0	0.31857	0.0	4.1
0.017544	0.38073	0.1	4.9
0.035088	0.439005	0.2	5.65
0.052632	0.512821	0.3	6.6
0.070175	0.595183	0.4	7.66
0.087719	0.714841	0.5	9.2
0.105263	1.048951	0.6	13.5
0.122807	1.622378	0.7	20.88
0.140351	2.205905	0.8	28.39
0.157895	3.003108	0.9	38.65
0.175439	3.994561	1.0	51.41
0.192982	5.060606	1.1	65.13
0.210526	6.00777	1.2	77.32
0.22807	6.28749	1.3	80.92
0.245614	6.658897	1.4	85.7

Table 3. Mechanical test data: Strain, Stress, Displacement, and Force for 200 mM 8% concentration

For this trial, it was observed that the Stress vs. Strain curve shows a linear region after the stress exceeds 1 Nm^{-2}. This linear region can be used to calculate the Young's Modulus as follows:

$$E = \frac{\sigma}{\varepsilon} = 47000 Nm^{-2}$$

When compared with the literature value of cardiac tissue, which was found to be around 10000 – 15000

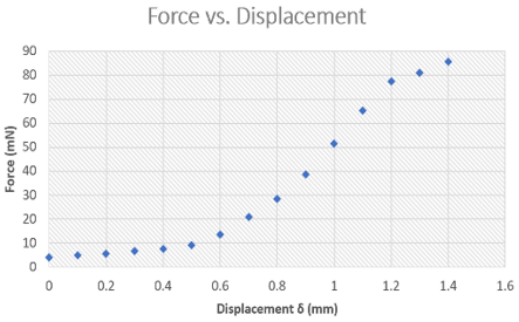

Figure 9A. Force vs. Displacement graph for 200 mM 8% concentration

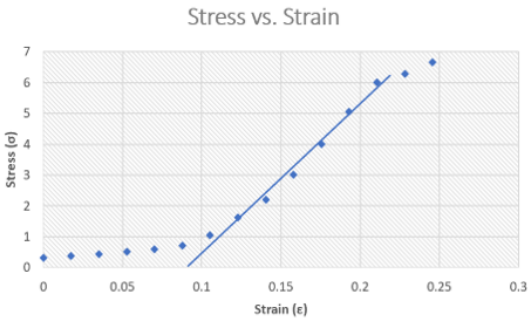

Figure 9B. Stress vs. Strain graph for 200 mM 8% concentration

Nm^{-2} [4], this sample composition of hydrogel appears to be too stiff to mimic the mechanical properties of a cardiac slice. Thus, the next step was to test a lower concentration (4 %).

2) Alginate Hydrogel Trial 2: 200 Mm 4% concentration of alginate

Due to the viscoelastic nature of hydrogels, they undergo stress relaxation under constant strain, meaning that the initial "maximum force" measured will gradually decrease to a lower "relax force" over time. This behavior closely mirrors biological tissues, which also exhibit viscoelasticity, and highlights why distinguishing between maximum and relaxed forces provides a more physiologically relevant assessment of material performance.

Displacement	Max Force	Relax Force	Stress Max (N)	Stress Relax (N)	Strain
0	-0.54	-0.54	-415.3846154	-415.3846154	0
1	2.919	1.96	2245.384615	1507.692308	0.01666667
2	6.32	4.944	4861.538462	3803.076923	0.03333333
3	10.306	8.36	7927.692308	6430.769231	0.05
4	14.65	11.4	11269.23077	8769.230769	0.06666667

Table 4. Force, Displacement, Stress and Strain Obtained from Mechanical Testing of 200 mM 4 % Alginate Hydrogel

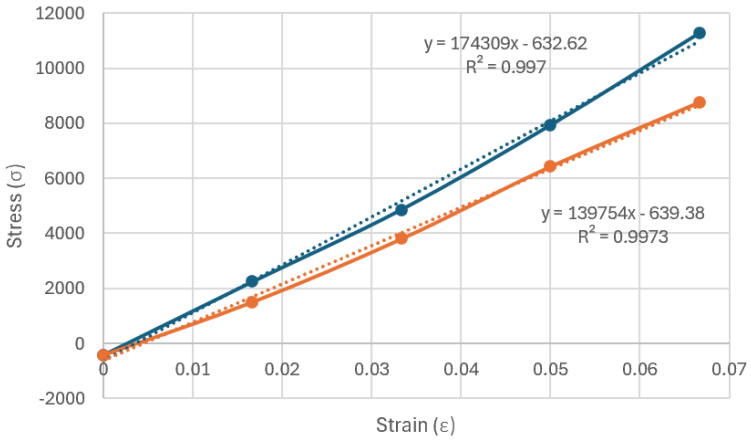

Figure 9. Stress Relax (orange) and Stress Max (blue) vs. Strain

The slope of Figure 9 (blue), the Stress Max vs. Strain graph, is slightly steeper than that of the Stress Relax vs. Strain (Figure 9, orange), yielding a higher value for Young's Modulus. This outcome is

expected, because in viscoelastic materials the initially measured "maximum" stress corresponds to the immediate elastic response of the network, whereas over time the material undergoes stress relaxation, resulting in a lower "relax" stress at the same strain. Consequently, the modulus derived from maximum stress will always be higher than that derived from the relaxed stress under these conditions. The relax values align well with the literature relaxed modulus of cardiac tissue, indicating that this concentration is a better synthetic model of a human cardiac slice.

4.3 Acoustic Patterning: Observations

As observed from the previously-conducted acoustic patterning procedure at the Huang Lab, acoustic frequency directly governs the resolution and density of cell patterning: higher frequencies (6.7 MHz) yield fine-scale cellular alignment with narrow inter-band spacing, while lower frequencies (2 MHz) produce coarser but denser multicellular assemblies. This tunability provides a means to tailor cell-laden constructs toward applications requiring either microscale anisotropy (e.g., modeling sarcomeric alignment) or macroscale tissue organization (e.g., engineered cardiac patches).

5 CONCLUSION

This study demonstrated the importance of optimizing hydrogel structural properties and strategically patterning cardiomyocytes for developing physiologically relevant in vitro models and environments for cardiac tissue. Mechanical testing of alginate hydrogels at different concentrations revealed that higher concentrations (8%) produced moduli well above the physiological stiffness range of native myocardium (10,000–15,000 Nm^{-2}). This would result in synthetic models that were too rigid to accurately mimic the cardiac microenvironment, and the hydrogels would be too viscous to allow movement of cells during acoustic patterning. In contrast, reducing the concentration to 4 % yielded stress–strain responses and Young's modulus values much closer to those reported for human cardiac tissue, highlighting this formulation as a more suitable scaffold for cardiomyocyte culture.

These findings are particularly significant in the context of cardiomyocyte maturation and function. Cardiomyocytes are highly mechanosensitive, and their structural alignment, contractility, and electrophysiological properties are strongly influenced by the stiffness of their extracellular matrix [7] [14]. By tuning hydrogel stiffness to match native myocardial tissue, it becomes possible to better support in vitro cardiomyocyte alignment, force generation, and long-term viability.

6 EVALUATION AND FUTURE STEPS

According to this study, alginate hydrogels with a lower concentration (4%) more closely resemble the myocardium's natural stiffness, while samples with higher alginate concentrations are too stiff to sustain cardiomyocyte activity, and samples with lower concentrations disintegrated during handling or weren't consistent enough to be cut into samples. Although the mechanical testing yielded useful estimates of modulus, there are still a number of limitations:

1. Limited datapoint density, baseline offsets, and lack of testing under physiological conditions reduce confidence in modulus estimates.
2. Non-homogenous samples with inconsistency in texture tested, due to the uneven nature of cross-linking when the $CaCl_2$ is released dropwise into the alginate mixture and PBS solution. The presence of clumps and incompletely cross-linked regions in the sample might have generated inaccuracies in data from tensile testing.
3. Cardiomyocyte viability, alignment, and functional maturation were not systematically assessed within the optimized hydrogel environment.

Future developments should therefore focus on improving the precision and reproducibility of mechanical testing, including viscoelastic characterization at 37 °C in physiologic media, and on standardizing hydrogel fabrication. Parallel efforts should optimize acoustic field parameters, quantify pattern fidelity, and assess cardiomyocyte outcomes through viability assays, structural maturation markers, and functional readouts such as contractility and conduction velocity. The modifications will enable the development of mechanically and structurally optimized hydrogel scaffolds capable of supporting physiologically relevant cardiomyocyte behaviour, advancing the utility of this system for cardiac disease modelling and regenerative medicine applications.

7 ACKNOWLEDGEMENTS

I would like to extend my gratitude to Dr. Shery Huang for supervising my research, reviewing my project proposal and report and allowing me to access the resources and support of The Huang Lab (Biointerface@CUED).

I am also grateful to Jack Murphy for directly overseeing this project and facilitating the procedure and testing of samples generated in the Cambridge Heart and Lung Institute at both the Cambridge Addenbrookes Site and the WestHub Nanoscience Centre.

REFERENCES

[1] BioRender (2025). Biorender illustrations. https://app.biorender.com/illustrations/canvas-beta/68821c92816cf5ff89ba866b. Accessed 16 Sept. 2025.

[2] Di Cesare, M. et al. (2024). The heart of the world. *Global Heart*, 19(1).

[3] Emig, R., Zgierski-Johnston, C. M., Timmermann, V., Taberner, A. J., Nash, M. P., Kohl, P., and Peyronnet, R. (2021). Passive myocardial mechanical properties: meaning, measurement, models. *Biophysical Reviews*, 13(5):587–610.

[4] Engler, A. J. et al. (2008). Mechanobiology of cardiomyocyte development. *PLoS ONE*, 3(3):e1528.

[5] Hoes, M. F., Bomer, N., and van der Meer, P. (2018). Concise review: The current state of human in vitro cardiac disease modeling: A focus on gene editing and tissue engineering. *STEM CELLS Translational Medicine*, 8(1):66–74.

[6] IonOptix (2025). Cardiac slice system - ionoptix. https://www.ionoptix.com/products/systems/cardiac-slice-system/. Accessed 12 Sept. 2025.

[7] Jacot, J. G., McCulloch, A. D., and Omens, J. H. (2008). Substrate stiffness affects the functional maturation of neonatal rat ventricular myocytes. *Biophysical Journal*, 95(7):3479–3487.

[8] Jorba, I. et al. (2021). In vitro methods to model cardiac mechanobiology in health and disease. *Tissue Engineering Part C: Methods*, 27(3):139–151. Accessed 12 Sept. 2022.

[9] Simons, E. et al. (2023). Ipsc-derived cardiomyocytes in inherited cardiac arrhythmias: Pathomechanistic discovery and drug development. *Biomedicines*, 11(2):334. Accessed 29 Mar. 2024.

[10] World Health Organization (2025). Cardiovascular diseases. https://www.who.int/health-topics/cardiovascular-diseasestab=tab$_1$.

[11] Wu, M. et al. (2024). Sound innovations for biofabrication and tissue engineering. *Microsystems & Nanoengineering*, 10(1). Accessed 19 Feb. 2025.

[12] Wu, P., Deng, G., Sai, X., Guo, H., Huang, H., and Zhu, P. (2020). Maturation strategies and limitations of induced pluripotent stem cell-derived cardiomyocytes. *Bioscience Reports*.

[13] Wu, Z. et al. (2022). Acoustofluidics for cell patterning and tissue engineering. *Engineered Regeneration*, 3(4):397–406. Accessed 15 Nov. 2022.

[14] Yeung, e. (2022). Substrate stiffness induces a chronic adaptation in contractile work and electrophysiology of cardiomyocytes. *Biophysical Journal*, ???(???):???